UDC 622.271:624.131.53/.54 DOI: https://doi.org/10.15407/geotm2026.176.126

Andrii Romanenko[1,*], https://orcid.org/0000-0002-8381-8873

[1]*Kryvyi Rih National University (KNU), Kryvyi Rih, Ukraine*
**Corresponding author e-mail:* romanencoa87@gmail.com

FRACTAL–STATISTICAL DETERMINATION OF THE STRUCTURAL WEAKENING COEFFICIENT OF A ROCK MASS

Abstract. Open-pit slope stability is controlled not only by intact rock strength but also by the spatial organization of fracture networks that subdivide the rock mass into blocks. In engineering practice the structural weakening coefficient is often assigned empirically, which limits the reliability of risk-oriented stability assessments. This study develops a fractal-statistical framework to refine the structural weakening coefficient k and to bridge 2-D fracture traces mapped on slope images with a 3-D appraisal of the rock-mass state. A grid of boxes with side length σ is overlaid on the fracture map, and $N(\sigma)$ denotes the number of boxes containing at least one fracture segment. The box-counting fractal dimension $D(B)$ is obtained from the slope of the ln $N(\sigma)$–ln$(1/\sigma)$ regression. To reduce sensitivity to grid placement and finite self-similarity ranges, the analysis incorporates a set of quality and heterogeneity descriptors: the coefficient of determination (R^2), standard error (*SE*), Y-intercept (*YINT*), prefactor, and the local non-uniformity index *S*. These parameters are embedded into an extended expression for the structural weakening coefficient *k* that complements the classical V/V_0 scaling and accounts for scale effects and spatial variability of jointing. Practical requirements for scale calibration and image resolution are outlined so the procedure can be repeated for routine and time-lapse surveys, enabling updates of the structural weakening coefficient k after blasting, weathering or seasonal changes. The approach is demonstrated for the Yeristovo open pit, where calculated fractal-statistical indicators are extrapolated to adjacent sectors considering lithology and structural trends, producing a zoning map of the structural weakening coefficient k for the whole pit wall. Zones with elevated $D(B)$ and unfavourable regression statistics (high *YINT* and *SE*, lower R^2, higher *S*) correspond to more fragmented and heterogeneous rock mass and therefore require enhanced monitoring, targeted inspections and conservative design assumptions. The proposed workflow provides a transparent, data-driven route to parameterise structural weakening for slope stability calculations and to prioritise hazardous sectors using routinely collected digital survey data.

Keywords: open-pit, slope stability, rock mass, fracturing, box-counting.

1. Introduction

The long-term stability of open-pit slopes is governed not only by rock strength but also by the spatial organisation of fractures that subdivide the rock mass into blocks. Traditionally, this influence is accounted for through a structural weakening coefficient, which is mostly assigned empirically; this limits the accuracy of risk-oriented slope stability calculations [1].

Fractal geometry provides a quantitative description of complex, scale-dependent fracture networks. Fractal dimension characterises how densely fractures occupy space across different scales, thereby linking laboratory-scale parameters to the behaviour of the rock mass at pit scale. Experimental studies and multifractal analyses of blasting products demonstrate a stable relationship between fractal dimension and the degree of rock damage [2–4].

Modern digital surveying techniques (photography, laser scanning, LiDAR, point clouds), combined with box-counting algorithms, enable the construction of maps of the fractal dimension of fracture traces. These descriptors have already been integrated with machine-learning methods to classify rock mass quality and assess its integrity [5].

At the same time, the relationship between fractal characteristics of fracturing and the structural weakening coefficient remains insufficiently defined. Weakening estimates are often based on simplified indicators such as fracture spacing and block

Received: 22.10.2025 Accepted: 15.12.2025 Available online: 31.03.2026

size, without accounting for the fractal nature of the fracture network [1–3]. This hampers the adoption of fractal analysis in practical open-pit slope design.

The aim of this study is to refine the structural weakening coefficient k as a linking element between the ratio V/V_0 and an integrated set of fractal and statistical parameters of fracturing derived from digital slope images using the box-counting method. This enables a transition from local two-dimensional fracture descriptors to a three-dimensional appraisal of the rock-mass state and allows k to be used as an informative parameter in open-pit slope stability calculations [6–8].

2. Methods

Quantifying fracture-network complexity on open-pit slopes is a practical task for stability assessment, hazard zoning, and routine geotechnical monitoring, especially under conditions of blasting, weathering, and seasonal changes that can rapidly modify rock-mass discontinuities [9, 10]. In this study, a fractal–statistical method is applied to derive an objective estimate of the structural weakening coefficient k from digital representations of slope surfaces.

A digital-survey workflow based on fracture-trace extraction and multi-scale box-counting analysis is proposed [9, 11–13]. The method is designed to determine the fractal dimension $D(B)$ of fracture patterns from slope photographs and photogrammetry-derived point-cloud products, and to evaluate the reliability of the obtained scaling law [11–14]. The procedure includes image/point-cloud pre-processing, contrast enhancement and noise suppression, delineation of fracture traces (binary mask), and repeated grid placement to reduce sensitivity to the initial position of the counting mesh.

To process the experimental data, a combined approach of fractal measurement and regression-quality control is used. The box-counting algorithm counts the number of occupied boxes N at a sequence of box sizes σ, and $D(B)$ is calculated from the slope of the $\ln N - \ln(1/\sigma)$ regression [14]. Alongside $D(B)$, the coefficient of determination (R^2), standard error (SE), Y-intercept ($YINT$), prefactor, and a local non-uniformity index (S) are computed to characterise both the scaling behaviour and spatial heterogeneity of fracturing. These descriptors are then incorporated into an extended expression for the structural weakening coefficient k, which complements the classical V/V_0 scaling and enables the transition from local 2-D fracture indicators to a 3-D appraisal of the rock-mass state and k-based zoning of the pit wall.

3. Theoretical and experimental parts

Fractal dimension provides a compact measure of fracture-network complexity; however, by itself it does not fully describe the reliability of the scaling law or the spatial variability of discontinuities that control mechanical behaviour. In practice, fracture traces extracted from images may contain noise, illumination artefacts, and limited self-similarity ranges, which can distort the $\ln N–\ln(1/\sigma)$ relationship and lead to unstable $D(B)$ estimates across different sectors and survey campaigns.

Therefore, fractal analysis should be complemented with statistical descriptors that quantify model fit, uncertainty, and heterogeneity. Regression-quality metrics (e.g., R^2, *SE*, *YINT*) help to verify whether the observed scaling is robust within the selected scale range, while parameters such as the prefactor and local non-uniformity index (S) capture differences in fracture density and clustering that may be critical for identifying potentially hazardous zones. Joint use of fractal and statistical indicators allows the structural weakening coefficient k to be derived in a more objective, reproducible, and engineering-relevant manner.

Six key parameters are employed to evaluate structural weakening of the rock mass due to fracturing and to assess the accuracy of fractal-dimension estimation:

1. Fractal dimension (*D(B)*)
2. Coefficient of determination (R^2)
3. Standard error (*SE*)
4. Y-intercept (*YINT*)
5. Prefactor (P_f)
6. Local non-uniformity index (*S*)

These parameters were selected because they provide a comprehensive and robust assessment of fracture-network structure.

Fractal dimension (*D(B)*)**.** This is the primary parameter describing the degree to which fractures fill space. It quantifies the geometric complexity of fracturing, characterises scale invariance of fracture distribution, and serves as a key indicator for comparing different structures.

Coefficient of determination (R^2). This metric evaluates how well the mathematical model fits the measured data. A high R^2 indicates that the estimated fractal model adequately describes the real fracture structure, which is essential for validating the calculation.

Standard error (SE). SE characterises the scatter of the data around the regression line. A low SE indicates higher modelling precision and helps to avoid significant errors in the determination of fractal dimension.

Y-intercept (YINT). The intercept of the regression line with the *Y* axis helps to characterise the initial conditions of the fracture distribution. It provides insight into how structures develop at the micro-scale and reflects their initial density.

Prefactor (P_f)*.* This parameter describes a scaling characteristic of fracturing. It accounts for the influence of fracture size on its distribution and provides additional information about the physical properties of rocks that control fracture development.

Local non-uniformity index (S). This index is used to assess spatial irregularity of fracture distribution. It helps to identify zones with intensified fracturing as well as areas where fracturing is less developed, which is important for evaluating rock-mass stability.

Taken together, these parameters enable a deep and multi-aspect assessment of fracturing, providing both quantitative analysis and qualitative interpretation of the results.

The Y-intercept obtained from linear regression, together with its associated parameters, indicates the following:

- A high Y-intercept may point to a risk of local deformations or stress concentrations.

- A low Y-intercept often suggests a more uniform distribution of micro-structures, which promotes stability.

For the conditions of the Yeristovo open pit, the following classification of Y-intercept values is adopted. The Y-intercept (*YINT*) is classified according to its magnitude, which reflects the initial properties of the rock-mass structure. Based on examples of fractal analysis of geological rock masses, *YINT* values can be conditionally divided into the categories below:

1. Critical ($YINT > 1.0$)
   - Characteristic: Very high density or heterogeneity at the finest scale.
   - Interpretation:
     - Strong stress concentration within the structure.
     - Risk of instability development, active crack growth, or local failures.
   - Example: Rock masses with intense fracturing within tectonic fault zones.
2. High ($0.7 < YINT \leq 1.00$)
   - Characteristic: Significant heterogeneity or high initial fracture density.
   - Interpretation:
     - Potential for additional crack formation.
     - May indicate a risk of local deformations.
   - Example: Zones with numerous microcracks or elevated tectonic stresses.
3. Moderate ($0.4 < YINT \leq 0.70$)
   - Characteristic: Moderate fracture density and structural heterogeneity.
   - Interpretation:
     - The rock mass can sustain substantial loads without noticeable deformation.
     - More uniform distribution of micro-loads.
   - Example: Typical rock masses in stable geological settings.
4. Low ($0.2 < YINT \leq 0.40$)
   - Characteristic: Nearly uniform structure with a low density of heterogeneities.
   - Interpretation:
     - The rock mass is characterised by high stability.
     - Low risk of crack development.
   - Example: Rocks that have not undergone significant anthropogenic disturbance.
5. Very low ($YINT \leq 0.2$)
   - Characteristic: Highly homogeneous structure.
   - Interpretation:
     - The rock mass is practically free of fractures or structural defects.
     - Maximum resistance to external impacts.
   - Example: Slightly fractured rocks, e.g., igneous intrusions.

The estimation of fractal dimension depends on the position of the initial grid; therefore, the optimal grid for multifractal analysis is selected using a probability criterion. The probability distribution is determined by the number of pixels N contained in each i-th element of size ε required to cover the object:

$$P(i,\varepsilon) = N_{(i,\varepsilon)} / \sum_{i=1}^{N} N_{i,\varepsilon} . \tag{1}$$

Thus, $P(i,\varepsilon)$ is derived from the probability distribution of weights for all elements i as the element size ε varies.

$$\sum_{i=1}^{N} P(i,\varepsilon)^{Q=1} = 1; \tag{2}$$

$$\sum_{i=1}^{N} P(i,\varepsilon)^{Q=0} = N_{(\varepsilon)}, \tag{3}$$

where Q is an arbitrary exponent used to define multifractal scaling. It is typically a negative number; however, it should be selected with regard to the maximum Q value to be applied. For the evaluation of the open-pit area image, the following range was adopted: minimum −10 and maximum +10. Using the software, the optimal distribution (placement) of the overlaid grid was obtained. $D(Q)$ is the *general dimension*, i.e., an averaged value of the fractal dimension. The formula for determining the generalised dimension takes the form:

$$D(Q) = \tau(Q) / (Q-1), \tag{4}$$

where $\tau(Q)$ is the slope of the regression line (Fig. 1); in our case it equals 0.03.

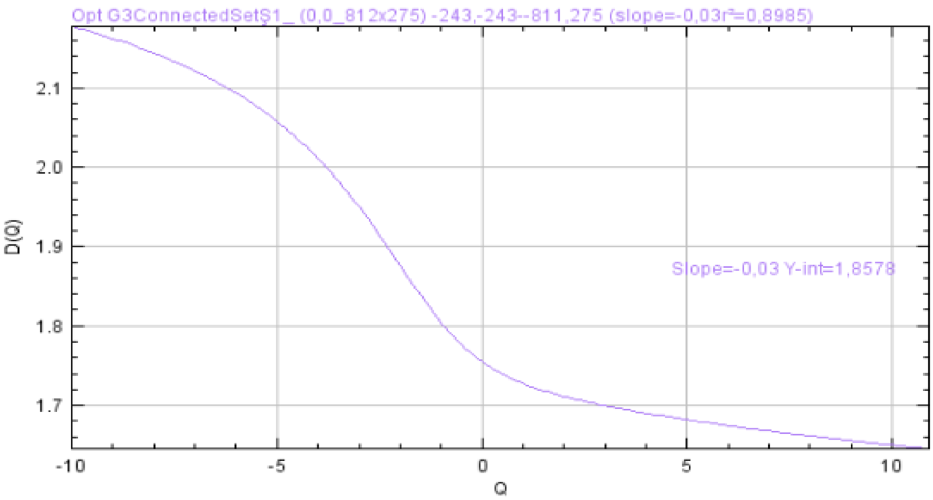

Figure 1 – Variation of $D(Q)$ with Q.

Thus, to obtain the most accurate assessment of fracturing within the analysed rock-mass sector, the grid takes the following configuration with an element size of 5×5 pixels. Figure 2a shows the general view of the sector, whereas Figure 2b presents a magnified fragment of the rock mass with the 5×5-pixel grid. Figure 2c illustrates a grid with an element size of 10×10 pixels. The grid overlay was performed over 15 iterations until the grid size reached a level that covers 30% of the vertical dimension of the image (Fig. 2d).

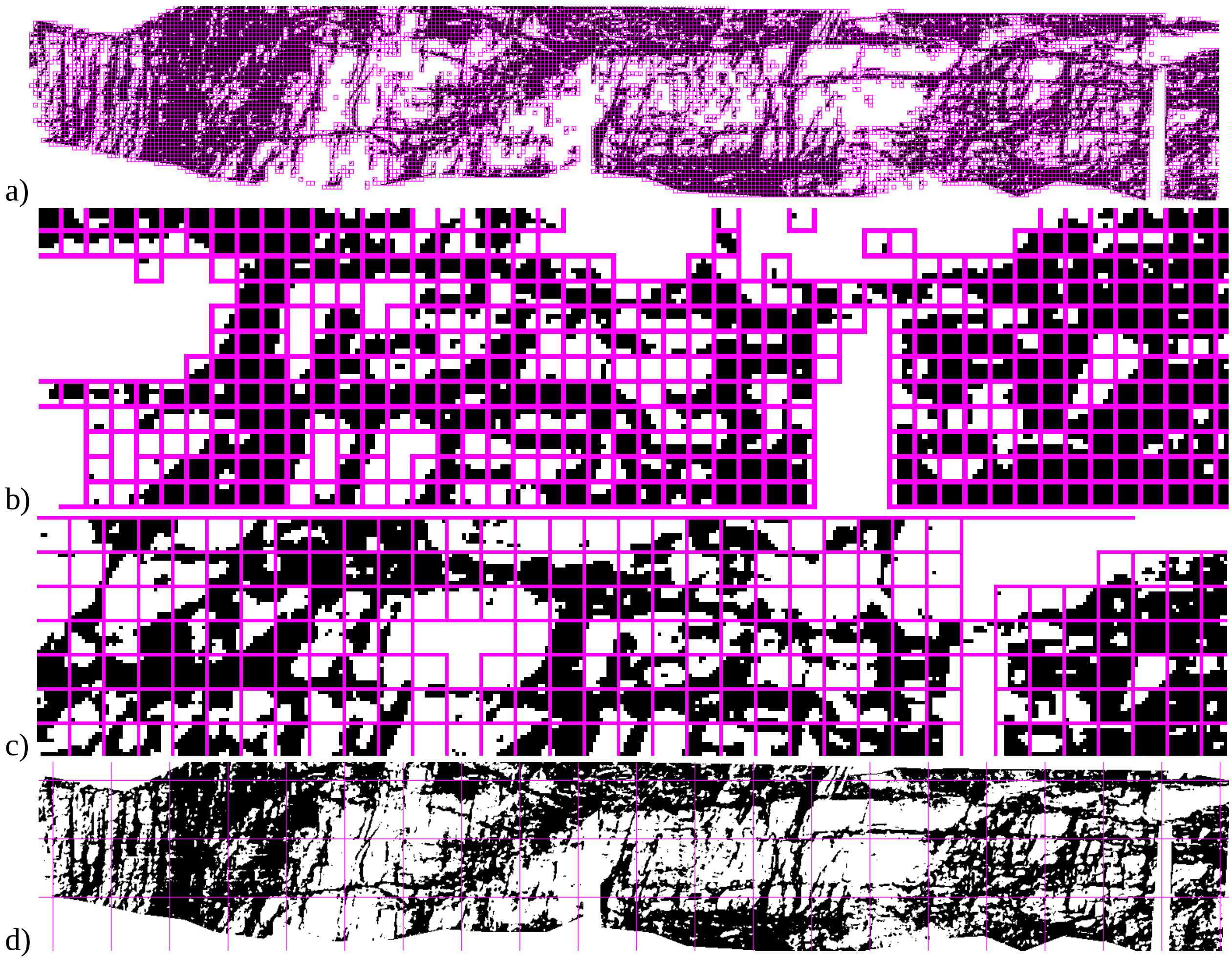

(a) General view of the sector with a 5×5-pixel grid overlay; (b) zoomed-in fragment of the rock mass with a 5×5-pixel grid; (c) zoomed-in fragment of the rock mass with a 10×10-pixel grid; (d) final grid-overlay iteration: the grid element covers 30% of the image's vertical dimension

Figure 2 – Multi-scale grid overlay used for box-counting analysis of the analysed rock-mass sector.

Nonlinear growth of the fractal dimension of discontinuities as a function of the applied load on a rock specimen.

The relationship is described by the following equation:

$$d = d_0 + \alpha \cdot (\sigma^2 - m \cdot \sigma), \quad (5)$$

where d_0 is the initial fractal dimension of the analysed rock-mass sector; α is an empirical scaling coefficient governing the intensity of the nonlinear increase in fractal dimension with increasing applied normal stress; m is an empirical coefficient; and σ is the applied normal stress.

In this way, the application of the above methodology makes it possible to obtain a quantitative estimate of the fractal dimension of rock masses based on the analysis of photographs of their slopes.

Using the fractal approach allows a more complete interpretation of the size effect in rock strength, which is expressed by the dependence of the failure strength σ_r (i.e., the limiting stress at which rupture occurs) on the geometric dimensions of the body [13, 14].

Given that, in a real solid, defects form a hierarchical structure, increasing the characteristic volume of a specimen raises the probability of the occurrence of a critical defect cluster within it. The intensity of this effect is described by the exponent m, which essentially reflects the material heterogeneity: at low m the structure is strongly "disturbed", whereas at high m it approaches a homogeneous state.

Further development of the model is based on the assumption that the ensemble of defects can be represented as a self-similar fractal cluster with fractal dimension d. In this case, the material heterogeneity coefficient is related to the fractal dimension of the defect subsystem: the larger the value of d, the more pronounced the strength size effect, and the lower the effective strength of large rock volumes. Comparing the limiting cases (nearly homogeneous material versus highly defective material) makes it possible to express the relationship between the strength of the real rock mass and that of an idealised intact rock as a function of d.

The ratio of the design stresses of intact rock to the stresses in the disturbed mass is interpreted as the structural weakening coefficient k_C. Substituting the fractal dimension into the corresponding power-law relationships and performing a logarithmic transformation yields an expression in which k_C is directly linked to the fractal dimension of the fracture structure. Hence, we obtain a formula for determining the structural weakening coefficient of the rock mass as a function of its fractal dimension [15]:

$$k_C = 10^{(2-d)\cdot lg\frac{V}{V_0}}. \tag{6}$$

To transition from an image-based description to a three-dimensional appraisal of the rock mass, it is necessary to account for scale effects and spatial features of the fracture structure, which are represented by the ratio of the rock volume within the potential sliding prism V to the rock volume of a characteristic structural block V_0. This ratio is expressed by the coefficient k, which makes it possible to generalise local two-dimensional parameters for evaluating the three-dimensional state of the rock mass. The use of k is essential because it incorporates the influence of physical and statistical characteristics of the rock that cannot be captured solely by the V/V_0 ratio;

therefore, the formulation is refined by introducing additional parameters, resulting in the following equation:

$$\frac{V}{V_0} = k = \frac{10^{(R^2 \cdot log_{10}(P_f + 1) + (Y\,int))}}{1 + SE + S}. \tag{7}$$

This equation enables an accurate transition from a two-dimensional assessment of fracture structure to its three-dimensional prediction, preserving scale invariance while incorporating key statistical parameters.

After determining all required parameters, a zonal distribution of the structural weakening coefficient is performed by extrapolating (approximating) the fractal-dimension results obtained for individual zones to adjacent sectors. In doing so, the geological–lithological composition of the rocks and the spatial variation of fracturing across the entire open pit are taken into account. This approach makes it possible to integrate local fractal-dimension indicators at the scale of the whole deposit. The zonal distribution of the structural weakening coefficient is shown in Fig. 3**.**

○ – sample collection points; ▭ – sectors denote the analysed zones, the short line attached to each sector indicates the viewing direction and photograph position;
“Zone No.” is the zone identifier, the numerical value inside each zone is the structural weakening coefficient k

Figure 3 – Zonal distribution of the structural weakening coefficient

Thus, the proposed refinement of *k* and the consistent linkage between the geometry of the fracture network derived from digital slope data form an integrated engineering–mathematical assessment of the structural weakening of the rock mass. Combining the fractal description of discontinuities with statistical indicators of regression quality and spatial heterogeneity enables reproducible *k*-based zoning of the pit wall and provides a basis for regularly updating the input parameters of stability calculations as mining operations progress.

The obtained values of *k* fall within the range 0.017–0.054, indicating pronounced heterogeneity of jointing and, consequently, structural disturbance of the rock mass.

The minimum values (approximately 0.017–0.021) delineate relatively "intact" zones, whereas the maximum values (approximately 0.051–0.053) correspond to areas with increased intensity/complexity of the fracture network. The map shows an evident clustering of elevated *k* values within several blocks (with a concentration of local "peaks"), which is consistent with the presence of structural heterogeneities and zones of intensified fracturing that may be regarded as potentially more hazardous in terms of degradation of strength properties.

From an interpretative standpoint, an increase in *k* reflects an increase in structural weakening; therefore, the resulting zoning can be used to rank areas by priority for parameter refinement and engineering decision-making (enhanced monitoring, more conservative assumptions, local stabilisation measures, etc.). In addition, within this study, laboratory refinement of the physical and mechanical properties of the rocks was performed, and the factor of safety was determined based on data obtained at the preceding stages; the derived *k* values were directly incorporated into numerical modelling using the MIDAS GTS NX software package (finite-element modelling of geotechnical problems).

4. Conclusions

This study presents a fractal–statistical workflow for characterising fracture-network complexity on open-pit slopes and for obtaining a more objective estimate of the structural weakening coefficient *k* from routine digital survey products. The proposed concept supports stability assessment and hazard zoning by translating geometrical information extracted from slope-surface data into an engineering parameter suitable for design and monitoring updates.

Fracture patterns are quantified using multi-scale box-counting applied to slope photographs and photogrammetry-derived point-cloud products. The fractal dimension *D(B)* is determined from the $\ln N$–$\ln(1/\sigma)$ scaling regression, while the reliability of the scaling law is controlled through a set of complementary descriptors (R^2, *SE*, *YINT*, prefactor, and the local non-uniformity index *S*). This combination reduces sensitivity to grid placement, limited self-similarity ranges, and image/point-cloud artefacts, and it provides an interpretable measure of spatial heterogeneity of discontinuities.

An extended *k* formulation is introduced to complement the classical V/V_0 scaling by embedding the above fractal and statistical indicators. As a result, the method enables a consistent transition from local 2-D fracture-trace metrics to a 3-D appraisal of rock-mass condition and provides a transparent basis for comparing slope sectors and survey epochs.

The workflow is demonstrated for the Yeristovo open pit (Ferrexpo Yeristovo Mining, FYM), where the calculated indicators are used to produce a zoning scheme of *k* along the pit wall, accounting for lithology and structural trends. Sectors characterised by higher *D*(*B*) together with unfavourable regression statistics (higher *YINT* and *SE*, lower R^2, higher *S*) correspond to a more fragmented and heterogeneous rock mass and should be prioritised for enhanced monitoring, targeted inspections, and conservative stability assumptions.

Future work should focus on expanding the database via time-lapse surveys (e.g., before/after blasting and across seasonal periods), validating *k*-zoning against independent geotechnical observations, and integrating the workflow into routine risk-oriented slope management.

Conflict of interest

Authors state no conflict of interest.

REFERENCES

1. Liu W., Sheng G., Kang X., Yang M., Li D. and Wu S. (2024), "Slope Stability Analysis of Open-Pit Mine Considering Weathering Effects", *Applied Sciences*, 14(18), 8449. https://doi.org/10.3390/app14188449

2. Pan C., Liu C., Zhao G., Yuan W., Wang X. and Meng X. (2024), "Fractal Characteristics and Energy Evolution Analysis of Rocks under True Triaxial Unloading Conditions", *Fractal and Fractional*, 8(7), 387. https://doi.org/10.3390/fractalfract8070387

3. Xiao C., Yang R., Ma X., Wang Y. and Ding C. (2024), "Damage Evaluation of Rock Blasting Based on Multi-Fractal Study", *International Journal of Impact Engineering*, 188, 104953. https://doi.org/10.1016/j.ijimpeng.2024.104953

4. Ma J., Li T., Shirani Faradonbeh R., Sharifzadeh M., Wang J., Huang Y., Ma C., Peng F. and Zhang H. (2024), "Data-Driven Approach for Intelligent Classification of Tunnel Surrounding Rock Using Integrated Fractal and Machine Learning Methods", *Fractal and Fractional*, 8(12), 677. https://doi.org/10.3390/fractalfract8120677

5. Liu H.-W., Chen S.-J., Xu Y.-J., Zhang X. and Bao X.-K. (2024), "Mapping Reconstruction of Rock Mass Fracture Based on Weierstrass-Mandelbrot Function", *Rock and Soil Mechanics*, 45(10), pp. 3058–3070. https://doi.org/10.26599/RSM.2024.9436722

6. Basirat, F., Aminnayeri, M. and Mirshafiei, M. (2019), "Determination of the Fractal Dimension of the Fracture Network in a Rock Mass Using Digital Image Processing", *Fractal and Fractional*, vol. 3(2), 17. https://doi.org/10.3390/fractalfract3020017

7. Mammoliti, E., Pepi, A., Fronzi, D., Morelli, S., Volatili, T., Tazioli, A. and Francioni, M. (2023), "3D Discrete Fracture Network Modelling from UAV Imagery Coupled with Tracer Tests to Assess Fracture Conductivity in an Unstable Rock Slope: Implications for Rockfall Phenomena", *Remote Sensing*, vol. 15(5), 1222. https://doi.org/10.3390/rs15051222

8. Kemeny, J. and Post, R. (2003), "Estimating three-dimensional rock discontinuity orientation from digital images of fracture traces", *Computers and Geosciences*, vol. 29, no. 1, pp. 65–77. https://doi.org/10.1016/S0098-3004(02)00106-1

9. Tong, X., Liu, X., Chen, P., Liu, S., Luan, K. and Li, L. (2015), "Integration of UAV-Based Photogrammetry and Terrestrial Laser Scanning for the Three-Dimensional Mapping and Monitoring of Open-Pit Mine Areas", *Remote Sensing*, vol. 7, no. 6, pp. 6635–6662. https://doi.org/10.3390/rs70606635

10. Pashchenko, O., Zabolotna, Yu., Koroviaka, Ye. and Rastsvietaiev, V. (2025), "Application of drone-based photogrammetry for monitoring surface deformation in open-pit mines", *Mining Science*, vol. 81, pp. 74–85. https://doi.org/10.33271/crpnmu/81.074

11. Riquelme, A., Abellán, A., Tomás, R. and Jaboyedoff, M. (2018), "Automatic mapping of discontinuity persistence on rock masses using 3D point clouds", *Rock Mechanics and Rock Engineering,* vol. 51, pp. 3005–3028. https://doi.org/10.1007/s00603-018-1519-9

12. Lato, M.J. and Vöge, M. (2012), "Automated mapping of rock discontinuities in 3D lidar and photogrammetry models", *International Journal of Rock Mechanics and Mining Sciences*, vol. 54, pp. 150–158. https://doi.org/10.1016/j.ijrmms.2012.06.003

13. Li X., Chen Z., Chen J. and Zhu H. (2019), "Automatic characterization of rock mass discontinuities using 3D point clouds', *Engineering Geology*, 259, 105131. https://doi.org/10.1016/j.enggeo.2019.05.008

14. Douglass, R.W. (2025), "Automated Box-Counting Fractal Dimension Analysis: Sliding Window Optimization and Multi-Fractal Validation", *Fractal and Fractional*, vol. 9, no. 10, 633. https://doi.org/10.3390/fractalfract9100633

15. Sydorenko V.D., Romanenko A.O. and Panchenko V.V. (2021), "Development of a methodology for determining the stability margin of an iron ore pit side section", *Collection of Research Papers of the National Mining University*, 64, pp. 68–80. https://doi.org/10.33271/crpnmu/64.068

ФРАКТАЛЬНО-СТАТИСТИЧНИЙ ПІДХІД ДО ВИЗНАЧЕННЯ *КОЕФІЦІЄНТА СТРУКТУРНОГО ОСЛАБЛЕННЯ ГІРНИЧОГО МАСИВУ*

Романенко А.О.

Анотація. Стійкість укосів кар'єру визначається не лише міцністю непорушеної породи, а й просторовою організацією мереж тріщин, що розчленовують гірський масив на блоки. В інженерній практиці коефіцієнт структурного ослаблення часто задається емпірично, що обмежує надійність ризик-орієнтованих оцінок стійкості. У роботі розроблено фрактально-статистичний підхід до уточнення коефіцієнта структурного ослаблення k та поєднання 2-D слідів тріщин, відображених на зображеннях укосів, із 3-D оцінкою стану гірського масиву. На карту тріщин накладається сітка комірок зі стороною σ, а $N(\sigma)$ позначає кількість комірок, що містять щонайменше один фрагмент тріщини. Фрактальна розмірність за методом box-counting $D(B)$ визначається за нахилом регресії ln $N(\sigma)$–ln$(1/\sigma)$. Щоб зменшити чутливість до розміщення сітки та скінченних діапазонів самоподібності, аналіз включає набір показників якості та неоднорідності: коефіцієнт детермінації (R^2), стандартну похибку (*SE*), перетин з віссю *Y* (*YINT*), префактор і локальний індекс неоднорідності *S*. Ці параметри вбудовано в розширений вираз для коефіцієнта структурного ослаблення *k*, який доповнює класичне масштабування V/V_0 та враховує масштабні ефекти й просторову мінливість тріщинуватості. Практичні вимоги до калібрування масштабу та роздільної здатності зображень викладено так, щоб процедуру можна було повторювати для рутинних і повторних у часі знімань, забезпечуючи оновлення коефіцієнта структурного ослаблення *k* після вибухових робіт, вивітрювання або сезонних змін. Підхід апробовано для Єристівського кар'єру, де розраховані фрактально-статистичні показники екстраполюються на суміжні сектори з урахуванням літології та структурних трендів, що дає змогу побудувати карту зонування коефіцієнта структурного ослаблення *k* для всього борту кар'єру. Зони з підвищеними значеннями *D*(*B*) та несприятливою регресійною статистикою (високі *YINT* і *SE*, нижчі R^2, вищі *S*) відповідають більш фрагментованому й неоднорідному гірському масиву і тому потребують посиленого моніторингу, цільових обстежень і консервативних проєктних припущень. Запропонований підхід забезпечує прозорий, керований даними інструмент для параметризації структурного ослаблення в розрахунках стійкості укосів та пріоритизації небезпечних секторів із використанням даних цифрових знімань, що регулярно збираються.

Ключові слова: кар'єр, стійкість укосів, гірський масив, тріщинуватість, box-counting.